Eur Radiol (2005) 15: 1051–1059
DOI 10.1007/s00330-005-2689-x

Birgit B. Ertl-Wagner
Roland Bruening
Jeffrey Blume
Ralf-Thorsten Hoffmann
Brad Snyder
Karin A. Herrmann
Maximilian F. Reiser

Prospective, multireader evaluation of image quality and vascular delineation of multislice CT angiography of the brain

Received: 16 November 2004
Revised: 6 January 2005
Accepted: 11 January 2005
Published online: 19 March 2005

B. B. Ertl-Wagner (✉) ·
R.-T. Hoffmann · K. A. Herrmann ·
M. F. Reiser
Institute of Clinical Radiology,
Klinikum Grosshadern,
University of Munich,
Marchioninistr. 15,
81377 Munich, Germany
e-mail: B.Ertl-Wagner@t-online.de
Tel.: +49-89-70953620
Fax: +49-89-79360823

R. Bruening
Institute of Neuroradiology, Klinikum
Grosshadern, University of Munich,
Munich, Germany

J. Blume · B. Snyder
Center for Statistical Sciences,
Brown University,
Providence, RI, USA

Abstract The aim of this prospective, multireader trial was to investigate image quality and vascular delineation of cranial multislice CT angiography (MSCTA) to identify strengths and weaknesses of the method. Sixty consecutive patients underwent standardized cranial MSCTA. The mean estimated effective dose was 0.96±0.11 mSv. Three masked readers independently graded image quality parameters and vascular delineation on a 5-point scale. Vascular attenuation values and dose-length products were assessed quantitatively. Quantitative parameters were evaluated with a proportional odds regression model with bootstrapped standard errors to adjust the relevant standard errors for correlation within subjects and across readers. The non-parametric Wilcoxon sign-rank test was applied for quantitative measurements. Good to excellent ratings were observed regarding image quality parameters and vascular delineation. The delineation of veins was rated higher than that of arteries (OR 2.00). Smaller arterial segments were rated significantly less favorably than larger segments (OR up to 26.98). Moreover, the cavernous sinus, the C2 segment of the ICA and the communicating arteries demonstrated lower scores. Attenuation values were >240 HU and vessel-to-parenchyma ratios >7 in all vessels. Cranial MSCTA achieved high ratings regarding image quality and vascular delineation. Relative weaknesses were found in small arterial subsegments and in vessels in close topographical proximity to bone.

Keywords Multislice CT · CT angiography · Central nervous system · Brain

Introduction

The advent of multislice computed tomography (MSCT) has brought decisive advantages for CT angiography (CTA) [1–3]. CTA necessitates both a high spatial and a high temporal resolution in order to serve as an adequate diagnostic tool [2]. If spatial resolution is too low, the delineation of pathology and the depiction of small vessels are severely hindered. Moreover, with poor spatial resolution in the *z*-axis, step artifacts limit the usage of multiplanar reformations [4]. Poor temporal resolution, on the other hand, limits the delineation of the bolus of contrast medium in the vessels and thus severely reduces the volume that can be covered in a single CTA examination.

With the introduction of MSCT technology, it has now become possible to depict large areas at a previously unsurpassed spatial and temporal resolution—a crucial improvement for CT angiography of the brain, which renders it more competitive with MR angiography and catheter angiography [1, 3]. While CT angiography with a single slice CT made an assessment beyond the main stems of the intracranial arteries, e.g. the M1 segment of the middle cerebral artery, very difficult and oftentimes impossible, MSCT angiography may now offer non-invasive vascular imaging far

beyond the initial segments of the larger intracranial arteries [5–7].

It has previously been shown that MSCT allows the application of a single bolus of contrast medium to simultaneously achieve a contrast in both the arterial and the venous cerebral vessels [8, 9]. It has, moreover, been demonstrated that a routine unenhanced cranial CT could be performed 1.8 times faster with MSCT technology as compared with single slice CT (SSCT) technology and that posterior fossa artifacts could be significantly reduced [10]. Readers preferred native cranial CTs acquired with MSCT technique to those obtained with SSCT technology [10].

Ghaye et al. [11] demonstrated the superiority of chest MSCT angiography in identifying small subsegmental pulmonary arteries as compared to SSCT. A recent study by Kudo et al. [12] has moreover demonstrated the ability of MSCT to detect the anterior spinal artery and the artery of Adamkiewicz on contrast-enhanced CT of the abdomen.

However, little is known yet about the strengths and weaknesses of MSCT angiography of the brain. Uncertainty prevails regarding the image quality attainable and the spectrum of vascular segments that may be confidently delineated with the new technology. We therefore aimed to assess the image quality attainable with this new method in a prospective multireader study applying a standardized protocol. Moreover, we wanted to evaluate the vascular delineation of arterial and venous vessels and their respective subsegments in order to identify strengths and weaknesses of the technique. In addition, absolute attenuation values and radiation doses were to be assessed to gain an insight into the objective vessel-to-parenchyma ratios and the estimated effective patient doses required.

Materials and methods

Subjects and imaging

A total of 61 consecutive patients underwent MSCT angiography of the brain with a standardized protocol on a 4-slice MSCT (Siemens Volume Zoom, Siemens Medical Solutions, Erlangen, Germany). One patient was excluded from analysis due to a protocol violation; the patient had inadvertently received only 60 ml of contrast medium. Out of the remaining 60 patients, 29 were male and 31 female. The mean age was 50 years, the median age 54 years (range 17–88). Local Institutional Review Board (IRB) approval had been obtained prior to the commencement of the study; informed consent had been provided.

The following acquisition parameters were applied: 100 mAs, 120 kV, collimation of 4×1 mm with a table feed of 4 mm per rotation, rotation time 500 ms. A 120-ml aliquot of a non-ionic contrast medium with an iodine concentration of 300 mg/ml was injected into the right antecubital vein with a power injector at a flow rate of 3–4 ml/s. Data acquisition was started after a fixed delay of 35 s. None of the patients included in the study had a known medical history of cardiac output failure.

Inclusion criteria were a given clinical indication for CT angiography of the brain as stated both by the referring neurologist or neurosurgeon and the ability to comply to the CT angiographic examination. Exclusion criteria consisted of contraindications for iodinated contrast media, such as a known allergy to iodinated contrast media, renal insufficiency or pathological thyroid function tests.

Final diagnoses were established by a combination of the full clinical history of the patient, clinical follow-up, information obtained from additional imaging and a consensus reading of two radiologists. These two radiologists were not involved in the scoring as readers and were familiar with the full clinical history, additional imaging and the clinical follow-up of the patient. They were asked to review all cases and to establish a final diagnosis in consensus. Consensus was achieved among the two radiologists in all instances, rendering the involvement of a third radiologist unnecessary. Additional imaging was performed in 44 patients to achieve the final diagnosis. It consisted of MR imaging in 29 patients, DSA in six patients and follow-up native CT scans in nine more patients. Sixteen patients did not undergo additional imaging, all of which demonstrated normal findings of the intracranial vasculature on CT angiography.

The CT dose index (CTDI) and the dose length product (DLP) were assessed for each examination. The effective dose was estimated from the DLP according to the method of Hidajat et al. with the following equation [13]:

$$\text{Dose eff}\,[\text{mSV}] = \text{DLP} \times 0.0023$$

Image evaluation

The acquired images were reconstructed as thin-sliding maximum intensity projections (MIPs) in three planes with an increment of 3 mm. Data analysis was performed at a PACS workstation (MagicView; Siemens Medical Solutions, Erlangen, Germany).

Qualitative image scoring was performed independently by three staff radiologists with experience in CT angiography of the brain. Each reader was masked to the scores of the other readers. The readers were first asked to evaluate the delineation of vessels or vascular segments on a 5-point scale, with 5 corresponding to a vessel or vascular segment with an optimal delineation in its entire length and 1 corresponding to a vessel or vascular segment that cannot be identified at all. The readers were asked to rate each of the following vascular structures: C1 and C2 segments of the right and left internal carotid arteries, basilar artery, M1, M2 and M3 segments of the right and left middle cerebral artery, A1, A2 and A3 segments of the right and left anterior cerebral artery, P1, P2 and P3 segments of the right and left posterior cerebral artery, anterior communicating artery,

posterior communicating artery, circle of Willis in its entirety, pericallosal artery, superior sagittal sinus, inferior sagittal sinus, confluens sinuum, internal cerebral veins, right and left transverse sinus and cavernous sinus. A total of 6120 datapoints regarding the vascular delineation were obtained by the readers.

Each reader was additionally asked to rate overall image quality on a 5-point scale. On this scale, 5 corresponds to an excellent image quality, 4 to a good image quality, 3 to an adequate image quality, 2 to a marginally acceptable image quality, and 1 to an unacceptably low image quality. Each reader, moreover, subjectively evaluated vessel contrast on a 5-point scale. On this scale, 5 corresponds to excellent vessel contrast, 4 to good vessel contrast, 3 to adequate vessel contrast, 2 to marginally acceptable vessel contrast, and 1 to unacceptably poor vessel contrast. The readers also assessed image artifacts on a 5-point scale. On this scale, 5 corresponds to a complete absence of imaging artifacts; 4 corresponds to mild artifacts not interfering with diagnostic decision making; 3 corresponds to moderate artifacts slightly interfering with diagnostic decision making; 2 corresponds to pronounced artifacts interfering with diagnostic decision making; however, it is still possible to arrive at a diagnosis; and 1 corresponds to a situation in which artifacts completely hinder diagnostic decision making. A total of 540 data points regarding image quality parameters were assessed by the readers.

In addition, a quantitative image analysis was performed for each patient. Regions-of-interest (RoIs) were placed in consensus by two radiologists in the following vessels: C1 segments of the right and left internal carotid arteries, basilar artery, M1 segments of the right and left middle cerebral artery, superior sagittal sinus, confluens sinuum, and right and left transverse sinus. Moreover, an additional RoI with an area of approximately 2 cm^2 was placed in the left sided medullary center of the brain parenchyma cranial to the left lateral ventricle. Attenuation values in Hounsfield units were assessed for each RoI.

Statistical analysis

In assessing vascular delineation, several comparisons were of interest. We aimed to compare arteries to veins and small arterial subsegments to larger arterial subsegments. In each case, due to the ordinal nature of the vascular delineation scale, the comparisons were performed via a proportional odds multinomial regression model. In comparing the vascular delineation of arteries to veins, all vessels from all subjects were used in the comparison. This leads to two sources of correlation: the first is due to the three readers each reading the same studies leading to a within-subject correlation; the second corresponds to the correlation among vessels from each patient being scored by the same reader leading to a between reader correlation. In other words, scores for multiple vessels within a subject are correlated, and scores from different readers for a particular vessel are also correlated. Thus, this clustering had to be accounted for when reporting parameter estimates and odds ratios. Given the complex nature of the clustering, it is easiest to account for this correlation by deriving the model standard errors using a standard bootstrapping approach with 10,000 resamples, where selection occurred at the patient level [14]. Hence we avoid the potentially pain staking process of multilevel modeling in this context with the only limitation being that we are not able to estimate any correlation parameters.

The comparison of smaller arterial subsegments to larger arterial subsegments was performed in a similar manner. Here, an overall comparison of the first, second, and third segments of the anterior cerebral arteries (ACA), the middle cerebral arteries (MCA) and the posterior cerebral arteries (PCA) was performed.

The assumption of the proportional odds model is that the influence of explanatory variables is independent of the cut-point for the cumulative logit. In other words, for example, in the comparison of arteries to veins, the odds ratio for the probability of a grade of 5 versus the probability of a grade less than 5 is the same as the odds ratio for the probability of a grade of greater than or equal to 3 versus the probability of a grade of less than 3. For each of the two comparisons of interest, the odds ratios for a higher score versus lower score with bootstrapped 95% bias-corrected confidence intervals were reported. All computations were performed using Stata version 7.0.

In assessing attenuation values, interest centered again in comparing attenuation values for arteries to those of veins. To accomplish this, a Wilcoxon signed rank test of paired differences was performed for all pair-wise combinations of veins and arteries for HU absolute density values. The median paired difference (vein minus artery) and p value of the Wilcoxon signed rank test were reported. All computations were performed using S-Plus version 6.0.

Results

Out of the 60 patients included in the study, 37 had no pathologic findings of the vessels, while seven had intracranial arterial occlusions, three intracranial arterial stenoses, four venous vascular occlusions, five intracranial aneurysms or arteriovenous malformations (three pre- and two post-therapy), three had pathologic intracranial vessels due to intracranial neoplasms and one patient had a status post-extracranial–intracranial bypass. Out of the 37 patients without pathologic findings of the intracranial vessels, two were identified with an intracerebral hemorrhage both of which were post-traumatic in nature. Overall, seven patients were identified with signs of an elevated intracranial pressure (ICP); three of these had extensive, space-occupying cerebral infarctions (76-year-old female, 59-year-old male, 62-year-old male), two had a large intracerebral hemor-

rhage (69-year-old male and 72-year-old female), one had an extensive intracerebral neoplasm (47-year-old female) and one had a status post-SAH and surgical clipping of the aneurysm with signs of an elevated ICP and of severe vascular spasms.

Out of the 60 patients, 29 patients additionally underwent MR imaging to achieve the final diagnosis, six patients underwent DSA and nine more patients underwent follow-up native CT scans. Of the 16 patients who did not undergo additional imaging, all were demonstrated to have normal findings of the intracranial vasculature on CT angiography. All diagnoses were made correctly by the readers, as compared to the final diagnoses established by the consensus reading with full clinical information, additional imaging, if available, and clinical follow-up.

Image quality parameters were rated as follows: overall image quality was graded as an average of 4.2; the median was 4, range 2–5. Image artifacts were graded as an average of 4.1; the median was 4, range 3–5. The subjective vascular contrast was graded as an average of 4.5; the median was 5, range 2–5. In our setting, only one study was rated to have an overall image quality and a subjective vascular contrast of only 2. This was the study of the 37-year-old male patient with a status post-acute subarachnoid hemorrhage (SAH) and aneurysmal clipping, who displayed signs both of severe spasms of the intracranial arteries and of an elevated ICP. All other patients had a rating of the image quality parameters of 3 or above.

Tables 1 and 2 summarize the reader ratings of the delineation of the various intracranial arterial and venous vessels; mean values averaged over all cases and all readers with median values and ranges are provided.

Readers rated the venous vessels with a mean of 4.44 (median 4, range 2–5), while arterial vessels were rated with a mean of 4.19 (median 4, range 1–5). When the proportional odds ordinal regression model with bootstrapping was applied to these data, the odds ratio of arteries receiving a higher score than veins was 0.501 with a bootstrapped 95% bias-corrected confidence interval between 0.416 and 0.608. Conversely, the odds ratio for veins to receive a higher score than arteries was 2.00 with a bootstrapped 95% bias-corrected confidence interval between 1.64 and 2.40 veins were therefore about 2 times more likely to be rated higher than arteries. Parameter estimates for this model with bootstrapped standard errors are contained in Table 3.

Table 1 Assessment of vascular delineation of venous structures. Mean values, as well as median values and ranges, are provided for each vessel

	Mean	Median	Range
Superior sagittal sinus	4.69	5	3–5
Inferior sagittal sinus	4.71	5	3–5
Left transverse sinus	4.31	4	3–5
Right transverse sinus	4.47	5	3–5
Cavernous sinus	3.76	4	2–5
Confluens sinuum	4.62	5	3–5
Internal cerebral veins	4.50	5	2–5

Table 2 Assessment of vascular delineation of arterial structures. Mean values as well as median values and ranges are provided for each vessel. *ACA* anterior cerebral artery, *PCA* posterior cerebral artery, *MCA* middle cerebral artery, *ICA* internal carotid artery

	Mean	Median	Range
Basilar artery	4.52	5	3–5
Left C1 segment of ICA	4.64	5	3–5
Left C2 segment of ICA	3.88	4	2–5
Right C1 segment of ICA	4.64	5	3–5
Right C2 segment of ICA	3.90	4	3–5
Left M1 segment of MCA	4.70	5	3–5
Left M2 segment of MCA	4.27	4	2–5
Left M3 segment of MCA	3.83	4	2–5
Right M1 segment of MCA	4.75	5	2–5
Right M2 segment of MCA	4.28	4	2–5
Right M3 segment of MCA	3.87	4	2–5
Left P1 segment of PCA	4.64	5	3–5
Left P2 segment of PCA	4.03	4	2–5
Left P3 segment of PCA	3.54	4	2–5
Right P1 segment of PCA	4.60	5	2–5
Right P2 segment of PCA	3.98	4	2–5
Right P3 segment of PCA	3.51	3	2–5
Left A1 segment of ACA	4.65	5	3–5
Left A2 segment of ACA	4.27	4	2–5
Left A3 segment of ACA	3.86	4	1–5
Right A1 segment of ACA	4.67	5	2–5
Right A2 segment of ACA	4.27	4	2–5
Right A3 segment of ACA	3.78	4	1–5
Anterior communicating artery	3.86	4	2–5
Posterior communicating artery	3.83	4	2–5
Circle of Willis in entirety	3.99	4	2–5
Pericallosal artery	4.46	5	2–5

Table 3 Proportional odds ordinal regression model to compare vascular delineability of veins and arteries. Standard errors shown were calculated by bootstrapping 10,000 samples. Here in constructing the cumulative logits, the higher score is in the numerator

Parameter	Estimate	Bootstrap SE
Intercept 1	−0.153	0.1123
Intercept 2	1.937	0.9897
Intercept 3	5.048	1.3722
Intercept 4	8.391	0.9719
Reader 1	−0.085	0.0956
Reader 2	1.112	0.0962
Reader 3	0	N/A
Artery	−0.690	0.0955
Vein	0	N/A

Table 4 Proportional odds ordinal regression model to compare vascular delineability of larger versus smaller intracranial arteries. Standard errors shown were calculated by bootstrapping 10,000 samples. Here in constructing the cumulative logits, the higher score is in the numerator

Parameter	Estimate	Bootstrap SE
Intercept 1	−2.708	0.234[a]
Intercept 2	−0.047	1.370[b]
Intercept 3	3.021	1.491
Intercept 4	6.1824	1.125
Reader 1	0.040	0.138
Reader 2	1.941	0.225
Reader 3	0	N/A
Large	3.295	0.290
Medium	1.459	0.179
Small	0	N/A
Large*Reader2	−0.858	0.231
Medium*Reader2	−0.414	0.158

[a]Based on 6339 samples
[b]Based on 9853 samples

Generally, readers gave smaller vascular segments lower ratings than larger vascular segments. The first segments of the anterior cerebral arteries (ACA), the middle cerebral arteries (MCA) and the posterior cerebral arteries (PCA) were rated as a mean of 4.67 (median 5, range 2–5), while the second segments of the ACA, MCA and PCA were rated as a mean of 4.18 (median 4, range 2–5) and the third segments of the ACA, MCA and PCA as a mean of 3.73 (median 4, range 1–5). When the proportional odds ordinal regression model with bootstrapping was fit, high odds ratios were obtained for larger segments (compare also Table 4). In this setting, readers 1 and 3 had very similar odds ratios and are reported together, while reader 2 had differing odds ratios and is therefore reported separately; hence we did not group all readers in the model, leaving a reader interaction term. Nevertheless, all readers demonstrated highly significant differences between large and smaller segments favoring the larger vascular segments. For readers 1 and 3, an odds ratio of 26.98 was found when comparing the first versus the third subsegments with a bootstrapped 95% bias-corrected confidence interval between 15.20 and 46.74, while for reader 2 an odds ratio of 11.44 was found (bootstrapped 95% bias-corrected confidence interval 6.80–20.87). When the first subsegments were compared with the second subsegments, an odds ratio of 6.27 was found for readers 1 and 3 with a bootstrapped 95% bias-corrected confidence interval between 4.61 and 8.39, while for reader 2 an odds ratio of 4.02 was found (bootstrapped 95% bias-corrected confidence interval 2.75–6.27). When the second subsegments were compared to the third subsegments, an odds ratio of 4.30 was found for readers 1 and 3 with a bootstrapped 95% bias-corrected confidence interval between 3.11 and 6.22, while for reader 2 an odds ratio of 2.84 was found (bootstrapped 95% bias-corrected confidence interval 2.18–3.84). When individually analyzing the scores of the third arterial subsegments, four patients were identified with scores of 2 or lower. All of these patients again had signs of an elevated ICP due to a large, space-occupying infarction (n=2), an intracerebral hemorrhage (n=1) and a status post-SAH (n=1).

When the vascular ratings for the arteries of the circle of Willis were assessed, a mean rating of 4.25 was found for the ACA (median 4, range 1–4), while a mean rating of 4.28 (median 4, range 2–5) was demonstrated for the MCA and a mean rating of 4.05 (median 4, range 2–5) for the PCA. The posterior cerebral artery therefore scored slightly lower than the middle and the anterior cerebral arteries.

When evaluating vascular segments that scored comparatively low, the cavernous sinus, the C2 segments of the carotid arteries and the communicating arteries of the circle of Willis were identified. The cavernous sinus was rated as a mean of 3.76 (median 4, range 2–5) as compared to a mean rating of 4.55 (median 5, range 2–5) for the remainder of the venous vessels. The C2 segments of the carotid arteries

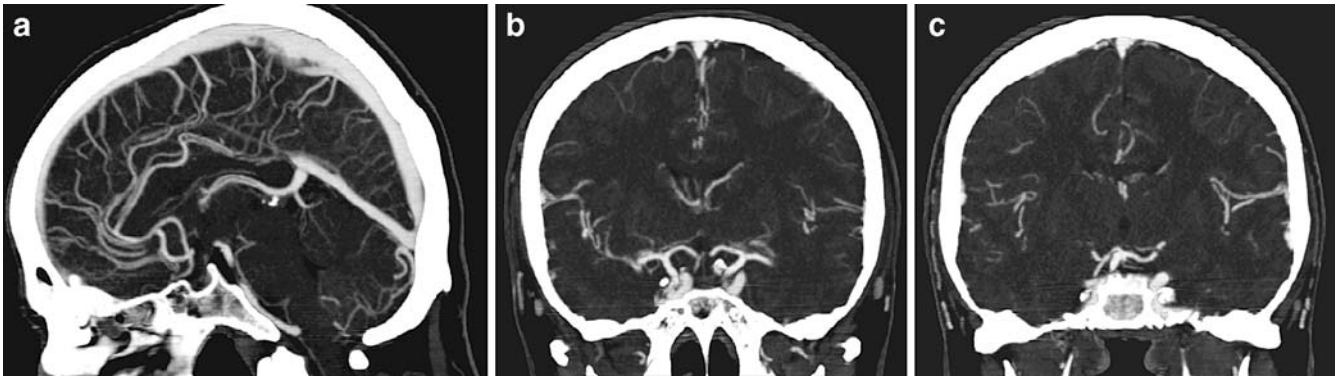

Fig. 1 Sagittal (**a**) and coronal (**b**, **c**) reformations of a MSCT angiography in a 48-year-old male patient without pathologic findings of the vessels. Both venous and arterial structures can be delineated well. Slight artifacts are noted especially in proximity to the skull base. Note that the small arterial subsegments, the cavernous sinus and the C2 segment of the ICA are more difficult to delineate

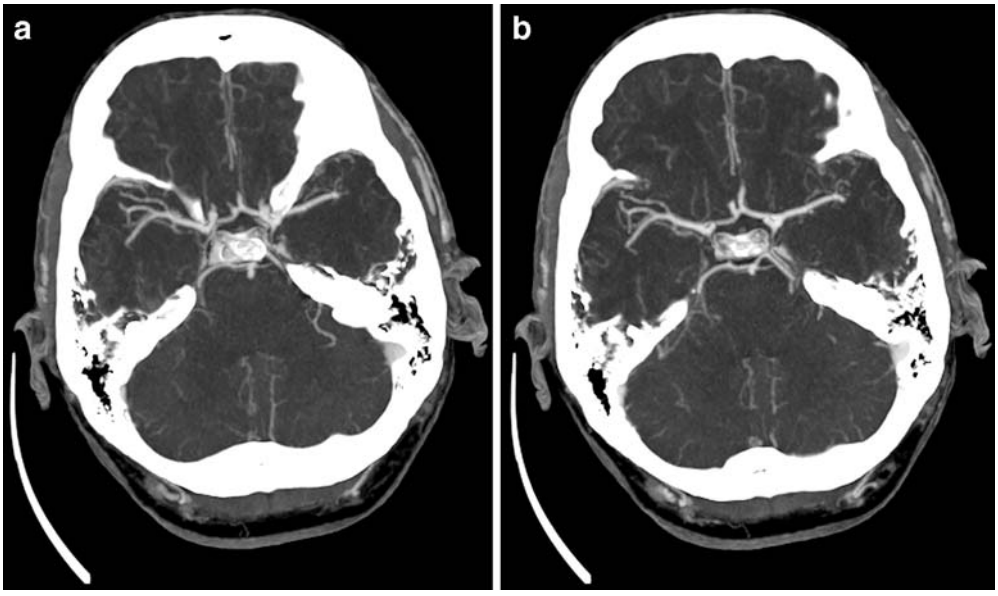

Fig. 2 **a**, **b** Axial reformations of a MSCT angiography in a 53-year-old male patient. The main stems of the circle of Willis can be delineated well. The small arterial subsegments and the vessels in proximity to bone are more difficult to delineate

were rated as a mean of 3.89 (median 4, range 2–5) as compared to a mean rating of 4.64 (median 5, range 3–5) of the C1 segments. Moreover, the communicating arteries of the circle of Willis were rated as an average of 3.84 (median 4, range 2–5) as compared to a mean rating of 4.25 (median 4, range 1–5) for the remainder of the arterial vessels.

Figures 1 and 2 demonstrate axial, coronal and sagittal thin sliding MIPs of MSCT angiographies in two patients. There is a high contrast of the vessels to the surrounding parenchyma and an excellent delineation of most vessels. The small subsegmental arteries, the cavernous sinus and the C2 segment of the ICA are more difficult to delineate, though.

Table 5 demonstrates the absolute attenuation values in Hounsfield units and the vessel-to-parenchyma ratios for the respective regions of interest. The mean attenuation both in the arterial and in the venous regions of interest was above 240 HU in all instances corresponding to a high intravascular opacification. Mean vessel-to-parenchyma ratios were above 7.0 for all regions of interest both in the arterial and in the venous system. The vessels were therefore at least 7 times as opacified as the deep white matter. When attenuation in the venous and arterial vessels were compared with a Wilcoxon rank test, there were no significant differences between the internal carotid arteries and the superior sagittal sinus and confluens sinuum, and between the basilar artery and the transverse sinus, corresponding to an even opacification between arterial vessels early in the course of the bolus transit and veins at a late stage of the contrast bolus. No differences were noted between the left and the right internal carotid arteries and the middle cerebral arteries. There were significant differences, though, when comparing the middle cerebral arteries and the basilar artery with the superior sagittal sinus and confluens sinuum with a higher opacification of the venous structures. There were also significant differences when comparing the internal carotid arteries to the transverse sinus with a higher attenuation of the arterial vessels (compare Table 6).

Analysis of radiation doses demonstrated a mean CTDI of 27.5 mGy and a mean dose length product of 417± 48 mGy cm. The mean effective dose was estimated to be 0.96±0.11 mSv for each CTA examination.

Table 5 Assessment of attenuation values and vessel-to-parenchyma ratios for selected regions of interest. Mean values and standard deviations are provided

	Mean attenuation (HU)	SD	Mean vessel-to-parenchyma ratios	SD
Superior sagittal sinus	278	72.2	8.16	2.4
Confluens sinuum	268	61.5	7.83	1.9
Right transverse sinus	259	62.6	7.55	1.9
Left transverse sinus	258	63.6	7.49	1.9
Basilar artery	253	68.9	7.39	2.0
Right internal carotid artery	278	73.8	8.10	2.2
Left internal carotid artery	277	68.1	8.15	2.4
Right middle cerebral artery	242	61.2	7.06	1.8
Left middle cerebral artery	248	64.4	7.25	2.0

Table 6 Wilcoxon signed rank test of paired differences for all pairwise combinations of veins and arteries for absolute attenuation values and vessel to parenchyma ratios. The median paired difference (vein minus artery) and *P*-value of the Wilcoxon signed rank test are reported (*P*-value is in parentheses) for each pairwise combination of vein and artery

	Basilar artery	Right ICA	Left ICA	Right MCA	Left MCA
HU absolute density values					
Superior sagittal sinus	27.5 (0.0003)	6 (0.664)	3 (0.7995)	36.5 (<0.0001)	32 (<0.0001)
Confluens sinuum	21.5 (0.004)	−7 (0.0667)	−9 (0.1037)	26.5 (<0.0001)	27 (0.0001)
Left transverse sinus	8 (0.1069)	−18 (0.0013)	−17.5 (0.005)	21 (0.0043)	12 (0.0362)
Right transverse sinus	8 (0.147)	−17.5 (0.0016)	−20.5 (0.0065)	16.5 (0.0047)	7 (0.0421)
Vessel to parenchyma ratios					
Superior sagittal sinus	0.822 (0.0003)	0.170 (0.6667)	0.085 (0.8081)	1.109 (<0.0001)	0.838 (<0.0001)
Confluens sinuum	0.599 (0.0042)	−0.202 (0.0736)	−0.261 (0.1007)	0.671 (<0.0001)	0.724 (0.0002)
Left transverse sinus	0.233 (0.1069)	−0.507 (0.0007)	−0.440 (0.0048)	0.574 (0.0048)	0.350 (0.0411)
Right transverse sinus	0.216 (0.136)	−0.536 (0.0015)	−0.536 (0.0058)	0.452 (0.0046)	0.217 (0.046)

Discussion

In our study of image quality and vascular delineation of MSCT angiography of the brain, we overall observed high scores regarding image quality parameters and vascular delineation.

When evaluating image quality parameters, we encountered a selective subset of seven patients with lower scores, all of which displayed signs of an elevated ICP due to a variety of causes. The diagnostic confidence was lower in this subgroup. Moreover, patients of the same subgroup had lesser scores of the subsegmental intracranial arteries, especially of the third subsegments. An elevation of the ICP therefore appears to interfere with image quality and especially with the analysis of small, subsegmental vessels, and to lower diagnostic confidence. This may in parts be a consequence of a reduced cerebral blood flow and an increasing constriction of the cerebral arteries in the situation of an elevated ICP [15–18].

When the vascular delineation attainable with MSCT angiography was assessed, our data demonstrate that venous vessels generally scored higher than arteries. This may in large part be a function of size, as the majority of the evaluated veins were larger than the arteries and their subsegments. Moreover, a relatively long delay may have added further to the relative superiority of the venous structures. The differences between arteries and veins were significant, but comparatively small with an estimated odds ratio of 2 for observing higher scores for veins over arteries. With average ratings of 4.44 for veins and 4.19 for arteries, the scores for vascular delineation were very high for both arterial and venous structures nevertheless.

When comparing the larger with the smaller segments of the arteries, highly significant differences could be demonstrated with very high odds ratios. Larger segments therefore scored significantly higher than smaller arterial subsegments. The confidence of vascular delineation decreased with a decreasing diameter of the vessel. However, scores of 1 or 2 were only observed among the subgroup of patients with an elevated ICP even in the third arterial subsegments. In the majority of patients, good or excellent vascular delineation was demonstrated even in the small arterial subsegments. MSCT angiography therefore appears to be able to depict even the small arterial subsegments with a high confidence, especially in the absence of an elevated ICP, even though larger arterial segments can be delineated significantly better.

As we aimed to identify strengths and weaknesses of the method, we assessed arterial and venous vessels that scored lower than the remainder. Besides the third subsegments of the ACA, MCA and PCA mentioned above, we identified the C2 segment of the ICA, the anterior and posterior communicating arteries and the cavernous sinus. We believe that the reason for a comparatively lower score of the anterior and posterior communicating arteries of the circle of Willis is most likely due to the small size, similar to the lower scores of the smaller subsegments of the ACA, MCA, and PCA. However, even the small arterial vessels could be reliably delineated and discerned by our readers. This is in accordance with a recently published study that demonstrated the accuracy of CT angiography in discerning a fetal origin of the posterior artery as a potential thrombo-embolic pathway [19]. The relatively poor score of the cavernous sinus and the C2 segment of the ICA is probably due to the close topographical proximity to the osseous structures of the skull base and constitutes a typical limitation of CT angiography. The high attenuation of both the contrast filled vessels and the bone makes differentiation difficult. Recently, matched mask bone elimination has been introduced into clinical practice [20–22]. A native CT scan is performed prior to CTA and then subtracted from the CT angiographic data leading to a similar image impression as in catheter DSA [20–22]. In our study, this novel technique was not applied yet. This technique may, however, prove to create a better delineation of the C2 segment of the ICA in the near future.

When we evaluated the absolute attenuation values and the vessel-to-parenchyma ratios of the various vascular

structures, we found no significant differences between the large vessels early and late in the course of the bolus of contrast medium, such as the ICA and the superior sagittal sinus, indicating a good timing of the bolus. There were differences, however, between arteries and veins with a higher score of the veins when comparing the superior sagittal sinus and confluens sinuum to the basilar artery and to the MCA and with a higher score for the arteries when comparing the ICA to the transverse sinus. The absolute magnitude of these differences was comparatively small, even though statistically significant. This again appears to be an effect of the size of the vessel and not of the timing of the contrast bolus as smaller vessels appear to have lower attenuation readings. This may be due to partial volume effects in the small arteries lowering the overall attenuation and to an increased difficulty placing the RoIs in small arteries with a higher likelihood of sampling errors [23–25]. Nevertheless, we were able to attain a very high attenuation throughout the study with a mean attenuation of at least 240 HU and a mean vessel-to-parenchyma ratio of at least 7 even in the small vessels.

Our evaluation of the dose lengths products of the examinations demonstrated a mean dose length product of 417 mGy cm and a mean estimated effective dose of 0.96 mSv for our MSCT angiographic examinations of the brain. According to the literature and to our own experience, a standard native cranial CT requires between 1.3 and 3.2 times this dose [26, 27]. We were therefore able to perform MSCT angiography with a low dose protocol, largely due to a low mAs product and an intermediate kV setting. In a recent study, a voltage setting of 120 kV has been demonstrated to be superior to a setting of 80 kV regarding image quality and the delineation of vacular structures, when the mAs product was kept constant [28]. In accordance with this study, we chose a kV setting of 120 kV for our study. There are some limitations to our study. First, we chose not to apply an individualized timing of the contrast bolus such as a test bolus or bolus tracking, since we intended to evaluate a protocol that can be easily performed in the daily clinical routine on a wide range of MSCT scanners. The use of a test bolus or of a bolus tracking method might have further increased the opacification and the homogeneity of the vessels. However, we were able to achieve a very high attenuation with high vessel-to-parenchyma ratios nevertheless. Moreover, we encountered no significant differences between the large vessels early and late in the course of the contrast bolus indicating a good timing. Our results therefore suggest that the use of a test bolus or of a bolus tracking may not even be necessary in a patient population without a history of congestive heart failure. This is in agreement with other studies of MSCT angiography of the brain that also applied a fixed delay to time the bolus of contrast medium [8, 9].

In addition, as indicated above, we chose a protocol with a comparatively low mAs product of 100 mAs in order to attain a low dose protocol. An increase of the mAs product to, for example, 200 mAs would have reduced the noise and would most likely have further increased the ratings both of the image quality parameters and of vascular delineation. This may have also increased the score of the areas that we identified as comparatively problematic such as the intraosseous portion of the ICA and the cavernous sinus. However, we were able to demonstrate that even a protocol with a low dose may attain very high ratings of image quality and vascular attenuation while simultaneously keeping the patient dose to a minimum. Moreover, it has previously been demonstrated in other organ systems that the mAs product may be reduced while still preserving an adequate image quality [29–31]. Further studies comparing the use of various mAs values for CTA of the brain will need to show whether a higher mAs setting may be able to even further increase vascular delineation of small vessels and of vessels in close proximity to bone.

As mentioned above, we moreover have not applied the matched mask bone elimination technique that has most recently been introduced into clinical practice. This technique may lead to a better delineation of the C2 segment of the ICA and of other structures in close topographical proximity to bone. Further studies will need to demonstrate whether this novel technique may in the future eliminate some of the current relative weaknesses of intracranial CT angiography.

In summary, we were able to demonstrate in our multireader evaluation of MSCT angiography of the brain that a very high image quality and vascular delineation can be achieved at a dose lower than that of a routine cranial CT. Both arteries and veins generally showed excellent ratings of their vascular delineation. Areas with comparatively lower quality were the third subsegments of the ACA, MCA and PCA, the communicating arteries of the circle of Willis, the intraosseous portion of the ICA and the cavernous sinus. Moreover, patients with signs of an increased ICP obtained lower scores.

We believe that MSCT angiography of the brain generally offers an excellent diagnostic tool to assess the intracranial arterial and venous vasculature at a low dose, if applied correctly. Caution should be exercised, though, when interpreting the small arterial subsegments, the communicating arteries, the intraosseous portion of the ICA and the cavernous sinus, and when evaluating scans in patients with an elevated ICP.

References

1. Rubin GD, Shiau MC, Schmidt AJ et al. (1999) Computed tomographic angiography: historical perspective and new state-of-the-art using multi detector-row helical computed tomography. J Comput Assist Tomogr 23(Suppl 1): S83–S90
2. Kalender WA, Seissler W, Klotz E, Vock P (1990) Spiral volumetric CT with single-breath-hold technique, continuous transport, and continuous scanner rotation. Radiology 176:181–183
3. Klingenbeck-Regn K, Schaller S, Flohr T, Ohnesorge B, Kopp AF, Baum U (1999) Subsecond multi-slice computed tomography: basics and applications. Eur J Radiol 31:110–124
4. Polacin A, Kalender WA, Marchal G (1992) Evaluation of section sensitivity profiles and image noise in spiral CT. Radiology 185:29–35
5. White PM, Wardlaw JM, Easton V (2000) Can noninvasive imaging accurately depict intracranial aneurysms? A systematic review. Radiology 217:361–370
6. Kato Y, Nair S, Sano H et al. (2002) Multi-slice 3D-CTA—an improvement over single slice helical CTA for cerebral aneurysms. Acta Neurochir (Wien) 144:715–722
7. Tomandl BF, Klotz E, Handschu R et al. (2003) Comprehensive imaging of ischemic stroke with multisection CT. Radiographics 23:565–592
8. Klingebiel R, Zimmer C, Rogalla P et al. (2001) Assessment of the arteriovenous cerebrovascular system by multi-slice CT. A single-bolus, monophasic protocol. Acta Radiol 42:560–562
9. Klingebiel R, Busch M, Bohner G, Zimmer C, Hoffmann O, Masuhr F (2002) Multi-slice CT angiography in the evaluation of patients with acute cerebrovascular disease—a promising new diagnostic tool. J Neurol 249:43–49
10. Jones TR, Kaplan RT, Lane B, Atlas SW, Rubin GD (2001) Single- versus multi-detector row CT of the brain: quality assessment. Radiology 219:750–755
11. Ghaye B, Szapiro D, Mastora I et al. (2001) Peripheral pulmonary arteries: how far in the lung does multi-detector row spiral CT allow analysis? Radiology 219:629–636
12. Kudo K, Terae S, Asano T et al. (2003) Anterior spinal artery and artery of Adamkiewicz detected by using multi-detector row CT. Am J Neuroradiol 24:13–17
13. Hidajat N, Maurer J, Schroder RJ et al. (1999) Relationships between physical dose quantities and patient dose in CT. Br J Radiol 72:556–561
14. Efron B, Halloran E, Holmes S (1996) Bootstrap confidence levels for phylogenetic trees. Proc Natl Acad Sci USA 93:13429–13434
15. Carmelo A, Ficola A, Fravolini ML, La Cava M, Maira G, Mangiola A (2002) ICP and CBF regulation: a new hypothesis to explain the "windkessel" phenomenon. Acta Neurochir Suppl 81:112–116
16. Acuff CG, Hoskins G, Moore NA, Rockhold RW (1996) Acute cerebral artery constriction in the spontaneously hypertensive rat following blood and plasma administration into the subarachnoid space. J Biomed Sci 3:117–125
17. Fukuhara T, Duoville CM, Eliott JP, Newell DW, Winn HR (1998) Relationship between intracranial pressure and the development of vasospasm after aneurysmal subarachnoid hemorrhage. Neurol Med Chir 38:710–715
18. Ertl-Wagner BB, Hoffmann RT, Bruening R, Herrmann K, Dichgans M, Reiser MF (2004) Blurring of the vessels of the interhemispheric fissure in multislice CT angiography: a sign of meningeal carcinomatosis. Eur Radiol 14:673–678
19. van der Lugt A, Buter TC, Govaere F, Siepman DA, Tanghe HL, Dippel DW (2004) Accuracy of CT angiography in the assessment of a fetal origin of the posterior cerebral artery. Eur Radiol 14:1627–1633
20. van Straten M, Venema HW, Streekstra GJ, Majoie CB, den Heeten GJ, Grimbergen CA (2004) Removal of bone in CT angiography of the cervical arteries by piecewise matched mask bone elimination. Med Phys 31:2924–2933
21. Venema HW, den Heeten GJ (2003) Subtraction helical CT angiography of intra- and extracranial vessels: technical considerations and preliminary experience-rediscovery of matched mask bone elimination? Am J Neuroradiol 24:1491 (author reply 1491–1492)
22. Venema HW, Hulsmans FJ, den Heeten GJ (2001) CT angiography of the circle of Willis and intracranial internal carotid arteries: maximum intensity projection with matched mask bone elimination-feasibility study. Radiology 218:893–898
23. Luboldt W, Weber R, Seemann M, Desantis M, Reiser M (1999) Influence of helical CT parameters on spatial resolution in CT angiography performed with a subsecond scanner. Invest Radiol 34:421–426
24. Polacin A, Kalender WA, Brink J, Vannier MA (1994) Measurement of slice sensitivity profiles in spiral CT. Med Phys 21:133–140
25. Imanishi Y, Fukui A, Niimi H et al. Radiation-induced temporary hair loss as a radiation damage only occurring in patients who had the combination of MDCT and DSA. Eur Radiol DOI 10.1007/s00330-004-2459-1
26. Huda W, Chamberlain CC, Rosenbaum AE, Garrisi W (2001) Radiation doses to infants and adults undergoing head CT examinations. Med Phys 28:393–399
27. Hamberg L, Rhea JT, Hunter GJ, Thrall JH (2003) Multi-detector row CT: radiation dose characteristics. Radiology 226:762–772
28. Ertl-Wagner BB, Hoffmann RT, Bruning R et al. (2004) Multi-detector row CT angiography of the brain at various kilovoltage settings. Radiology 231:528–535
29. Sohaib SA, Peppercorn PD, Horrocks JA, Keene MH, Kenyon GS, Reznek RH (2001) The effect of decreasing mAs on image quality and patient dose in sinus CT. Br J Radiol 74:157–161
30. Prasad SRWC, Shepard JA, McLoud T, Rhea J (2002) Standard-dose and 50%-reduced dose chest CT: comparing the effect on image quality. Am J Roentgenol 179:461–465
31. Garg K, Keith RL, Byers T, Kelly K, Kerzner AL, Lynch DA, Miller YE (2002) Randomized controlled trial with low-dose spiral CT for lung cancer screening: feasibility study and first results. Radiology 225:506–510